Research Papers
Issue RP0226
September 2014

ISC - Impacts on Soil and Coasts Division

Climate and Hydrological Data available for Climate Change Studies in China

By **Renata Vezzoli**
Impacts on Soil and Coasts Division, CMCC
renata.vezzoli@cmcc.it

Maria Paola Manzi
Impacts on Soil and Coasts Division, CMCC
mariapaola.manzi@cmcc.it

Nicola Ciro Zollo
Impacts on Soil and Coasts Division, CMCC
nicola.zollo@cmcc.it

and **Paola Mercogliano**
Impacts on Soil and Coasts Division, CMCC Division Meteo System & Instrumentation Laboratory, C.I.R.A.
p.mercogliano@cira.it

SUMMARY The present study summarised the dataset available used for climate and hydrological studies in China. The main aim is to identify the possible sources of climate and hydrological datasets to be used to validate the hydrological outputs of a GCM/RCM climate model and/or of a coupled climate/hydrological model. Furthermore a brief analysis of the state of art pubblications concerning the impact of climate changes on the hydrological hazards, such as floods and droughts, over some areas of China is also reported.

This activity has been conducted in the framework of WP B.1.6 of the GEMINA project.

Keywords: Climate and Hydrological datasets, China

The present research paper collects the outcomes of activities carried out in the framework of Work Package B.1.6 of the GEMINA project, funded by the Italian Ministry of Education, University and Research and the Italian Ministry of Environment, Land and Sea.

INTRODUCTION

According to the analysis carried on by the China Meteorological Administration, in the past century 1908-2007, the average temperature at the ground is increased of about 1.1°C with warmer winters in the more recent period and summer heat waves frequency is increased. At the same time, significant variations in the precipitation in the last half of XX century have been detected: precipitation increases in western and southern China and decreases in most parts of northern and northeaster China. Changes in precipitations reflects in an increase occurrence of heavy rainfall (southern China), snow related disaster (western China) and droughts (northern China) Additionally an increase in the sea temperature and level has been detected along Chinese coasts. Such phenomena are expected to intensify in frequency and severity in the next years [36]. According to the White Paper [36], the climate change has already caused changes in the distribution of water resources all over China, with a reduction of water resources of the rivers in northern China and a slight increase for those in southern China. The occurrence of floods is increased while droughts are becoming more severe. The temporal and spatial distribution of water resources is expected to be modify in an augment in the annual and inter-annual changes that fosters the occurrence of extreme natural disasters, including flood and drought. The melting of glaciers in western China will be accelerated with a consequent reduction of glaciers areas and ice reserves, that in turn will affect the discharge of ice-melting feed rivers. The positive drought trend in northern China is expected to continue and intensify water scarcity and contradiction between water supply and demand.

Within the action B of the project GEMINA, CMCC ISC Capua team is performing climate simulation over the Chinese region to investigate which areas and how they will be affected by climate change. The preliminary works to assess the capability of the regional climate model COSMO-CLM [38] to properly reproduce the recent climate of China before simulate the future are presented and discussed in [1, 2]. Here, we propose a literature review to identify the climate and hydrological datasets used in climate and hydrological studies over China and works concerning analysis of impact of climate changes on hydrological hazards. Once assessed the existence and extension of those dataset, the possibility to access to them to validate a hydrological model or the COSMO-CLM hydrological variables will be checked. In the next section we will list the climate and hydrological datasets used in the reviewed literature and try to describe their main features.

CLIMATE DATASETS

For climate studies on China several Authors use the observed timeseries collected, validated and distributed by the National Climatic Centre of the China Meteorological Administration, that also guaranteed the quality of the data released. The observed data include daily precipitation, air temperatures, wind speed, vapour pressure, radiation, and sunshine duration. This dataset is constantly updated since 1950-1960 and is composed by more than 700 meteorological stations [4, 30, 62, 55]. As web source to access observed climate data Chen et al. [5] indicate the China Meteorological Data Sharing Service System (http://data.cma.gov.cn). Observed data were used at daily [4, 9, 10, 11, 12, 13, 14, 15, 20, 19, 22, 21, 26, 25, 27, 30, 29, 41, 43, 44, 49, 59, 56, 62, 58], monthly [7, 23, 40, 46, 45, 55, 63] and yearly [5, 40, 59, 56] timescale. Figure 1(a) reports the location of the meteorological stations in China and of the main river basins and Fig.1(b) reports the location of the ten climate zones in which Chinese territory may be divided and in Tab.1 significant climate statistics for each zone are reported.

The second source of climate data to study Chinese climate and its changes are the NCEP/NCAR reanalysis (http://www.cdc.noaa.gov) from the National Centers for Environmental Prediction/National Center for Atmospheric Research (NCEP/NCAR) reanalysis, these data have been used e.g. by [16, 7, 18, 24, 32, 48, 51, 59]. The third source of climate data to study Chinese climate or to validate global and regional climate models outputs is the CRU [34] dataset. This data have been used by [1, 2, 17, 32, 42] to validate the outputs of GCM/RCM simulations. The CRU (Climate Research Unit) dataset developed by the University of East Anglia has been constructed from station data, collected by several sources, interpolated as a function of latitude, longitude and elevation using thin-plate splines with a horizontal resolution of 0.5° (about 60 km). It provides monthly estimates of several variables, like mean, minimum and maximum temperature, total precipitation amount and cloud cover. Other sources are the APHRODITE project [54] dataset to which refers [32, 42] to validate precipitation from the RCM REMO driven by ERA40 Reanalysis and the GCM ECHAM and the AE observation dataset developed by Xie et al. [50] this last one has been used by [16]; both validated versus other climate datasets by Sun et al. [42] that investigates the similarities and differences among some widely used gridded datasets for the Chinese area, see Table 2. The climate (meteorological) variables considered are the precipitation (PR) and the surface air temperature (SAT), for both variable a general agreement among the considered datasets is found on the whole spatio-temporal scale, see Fig. and Taylor diagrams 3. Since the EA dataset is based on more than 2200 gauge and CN05 on 751 stations they were used as reference for precipitation and temperature fields respectively on the control period 1970-1999. Figure shows the time series of annual mean precipitation and temperature among all datasets. Sun et al. [42] marked that, for precipitation, the datasets are in agreement after 1950 but they show a different trend before 1950: CRU dataset trend is 3.1 mm/decade; UDEL dataset -11.0 mm/decade and GPCC -13.8 mm/decade. The difference is justified by the reduced number of instrumental observations in the first half of the 20th century or the higher available of station observations after the 1950s [42]. For temperature, Sun et al. [42] find an undulating rise overall (Fig.(b)) but in different periods: the upward rates of temperature before the 1950s are small with a change rate values of CRU of 0.116 °C/decade and for UDEL of 0.146 °C/decade. Between 1951-1970, the IAP dataset shows a significant negative trend of about -0.9 °C/decade while in UDEL and CRU datasets only a slight decrease is evident: -0.15 °C/decade and -0.11 °C/decade, respectively. Temperatures rise again after the 1970s, with a rates of change of approximately 0.3 °C/decade. For the period 1962-2006 CRU and UDEL recorded a temperature higher than CN05 and IAP datasets. Overall, in the last 50 years all the precipitation and temperature datasets show a reasonable agreement each to the others. The Taylor diagram, Fig.3(a), displays the agreement of the 45 year annual mean climatology (PR and SAT) between the reference and other datasets. For precipitation, the high correlation coefficient, the similar values of standard deviation and root mean square difference proof the similarity of the datasets in term of annual precipitation dynamics. The precipitation datasets that more fit the

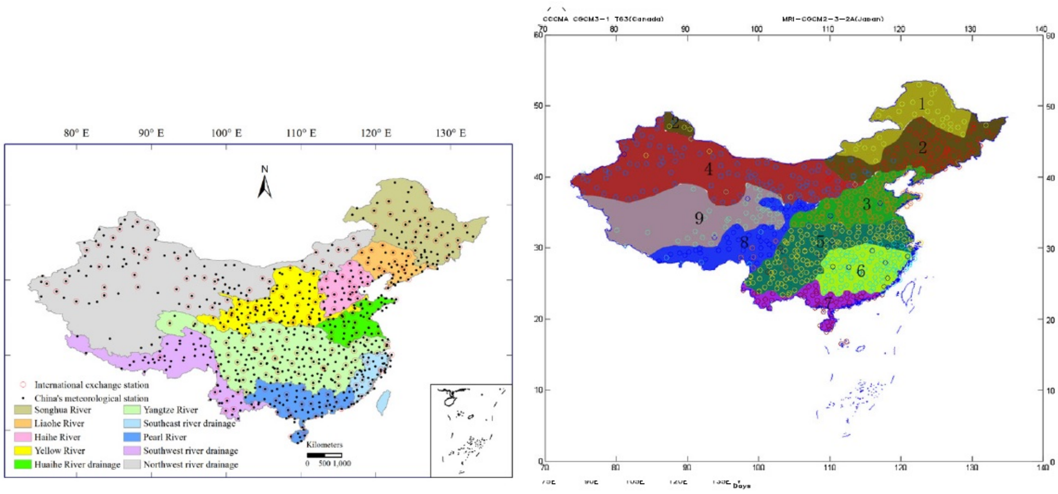

(a) (b)

Figure 1:
(a) Locations of meteorological stations and major river basins in mainland China. Source [42]. (b) Spatial distribution of climate zones. Numbers represent the different climate zones as reported in Tab. 1. Source [62].

Table 1
Altitude and climate characteristic of climate zone drawn in Fig.1(b), adapted from [62].

	Altitude (m)	Precipitation (mm)				Temperature (°C)			
Code Zone	Mean (Min-Max)	Spring	Summer	Autumn	Winter	Spring	Summer	Autumn	Winter
1 Temperate	632 (66.4-2458)	56.5	257.2	68.5	12.1	2.5	18.7	1.1	-20.1
2 Sub-humid warm temperate	508 (37-5496)	82.7	353.9	93.9	15.5	6.8	20.9	6.0	-12.4
3 Humid warm temperate	446 (2-7423)	107.1	376.0	134.4	29.8	12.6	24.0	13.1	-0.5
4 Arid warm temperate	1252 (34-3090)	33.8	94.1	36.3	9.7	10.0	22.0	7.9	-7.7
5 Northern subtropical	676 (3-2545)	242.5	516.0	233.4	75.4	16.2	24.6	16.8	6.6
6 Central subtropical	156 (5-1583)	546.6	556.5	230.3	198.8	17.4	27.1	19.5	8.3
7 Southern subtropical	252 (3-1414)	377.3	819.6	358.7	100.5	22.4	27.1	22.8	15.3
8 Plateau temperate	2878 (1347-4040)	99.2	316.7	126.8	15.3	6.6	14.6	6.3	-3.6
9 Plateau sub-frigid	3699 (1654-4800)	75.7	260.5	92.9	12.0	0.2	9.8	0.0	-11.1
10 Mountain climate	1672 (1164-3047)	553.9	776.5	369.3	192.5	9.6	18.5	10.8	0.7

reference one (EA) are IAP and GPCC, while UDEL and APHRO datasets are relatively less consistent with EA. For temperature, the Taylor diagram, Fig.3(b), shows that the agreement between CN05 and CRU is still better than that between CN05 and UDEL and the agreements of CRU and UDEL on temperature are better than that on precipitation. The 45 year average precipitation patterns are very similar among the datasets; in all the datasets the precipitation gradually decreases from the southeast to the northwest regions, however the datasets show different values for the maximum annual precipitation: about 2500 mm in APHRO, CRU and IAP); about 3930 mm in PREC/L, and about 5000 mm in GPCC, EA, and UDEL. THe EA, PREC/L, UDEL and GPCC datasets show heavy rainfall events across the southern Southwest river drainage system, such events do not appear in CRU, IAP and APHRO datasets. In general, the precipitation of all the datasets is lower of the one in EA in most parts of China, especially in the eastern Tibetan Plateau, particularly in CRU, GPCC, PREC/L and UDEL datasets, the northern Northwest river drainage system and southeastern China. For the 45 year average temperature, there is a good agreement in the patterns exhibited by the datasets; a little discrepancy is found in the eastern region. In the comparison to CN05, CRU shows a higher temperature in the central and southern Northwest river drainage basin, UDEL exhibits a higher temperature over the Southwest river drainage system, and IAP has a lower value in the Tibetan Plateau; a significant difference occurs in western China, where the largest topographic gradient exists. The results show that all datasets can succeed in exhibiting temporal changes in terms of precipitation and temperature and the characteristics of spatial patterns as a whole, however, there are some discrepancy, due to sample size and quality or to the interpolation method, that should be considered in using a dataset to validate a climate simulation.

HYDROLOGICAL DATASETS

For hydrological datasets the question is slightly more complex, from the Literature review it results that streamflow data are collected by each River Basin Authority [17, 8, 5, 25, 29, 51, 57] that made the data available, they are available from the Hydrological Yearbooks of the People's Republic of China [8, 23, 40, 61] or the National Meteorological Observatory [56]. A source to download the hydrological data is the Data-sharing Network of China Hydrology (http://www.hydrodata.gov.cn), [5], but it was not possible to access it since the site was temporarily out of service. The reliability and homogeneity of the hydrological data collected and published by Chinese authorities are checked for reliability and homogeneity before being released. Since global and/or regional climate models provide among the other outputs the runoff, this variable may be used to fed a hydraulic model to simulate river discharges, the comparison among simulated and observed discharges gives an indication of the capability of the climate model to reproduce the water cycle [3] e.g. the validation of RCM PRECIS [3] or Guo et al. [17] that uses the SWAT model to evaluate the impacts of climate and land-cover changes on streamflow in the Xinjiang River basin. Snow is an important component of the hydrological cycle, in this case satellite imaginery are a valid source of data combined with observations [28]; Zhang et al. [60] use a modified monthly degree-day model for evaluating glacier runoff changes in China and [65] simulated cold regions hydrological processes using the modular model Cold Regions Hydrological Model platform that permit to evaluate the importance of snow energy balance, blowing snow and frozen soil infiltration processes

Table 2

Datasets used in Sun et al. [42]; adapted from [42].

Dataset	Variable	Spatial domain	Temporal domain	Reference
EA (East Asia)	PR	0.5° East Asia	1962-2006 daily	[50]
CN05 (National Meteorological Information Center, China)	SAT	0.5° China	1961-2008 daily	[52]
APHRO (Asian Precipitation Highly Resolved Observational)	PR	0.5° Asia	1951-2007 Daily	[53, 54]
CRU (Climate Research Unit)	PR, SAT	0.5° global	1901-2009 Monthly	[35]
GPCC (Global Precipitation Climatology Centre)	PR	0.5° global	1901-2010 Monthly	[39]
PREC/L (precipitation reconstruction over land)	PR	0.5° global	1948-2011 Monthly	[6]
UDEL (University of Delaware)	PR, SAT	0.5° global	1901-2010 Monthly	[47]
IAP (Institute of Atmospheric Physics, China)	PR, SAT	0.5° China	1951-2007 Monthly	[64]

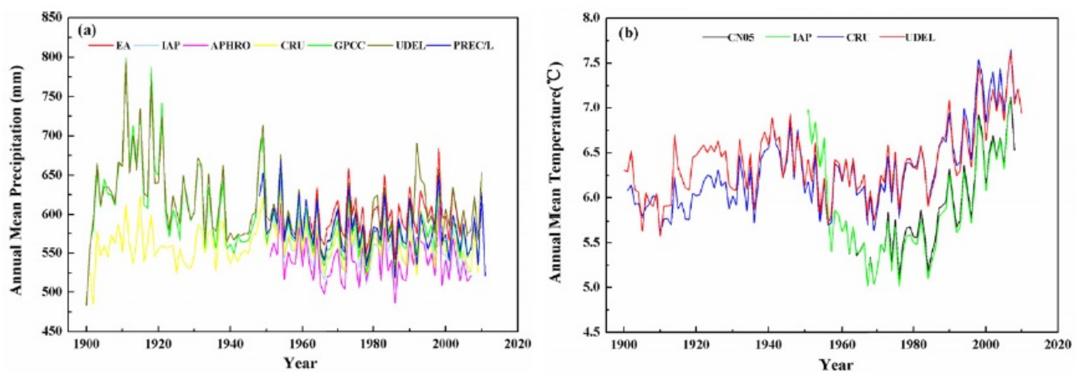

(a) (b)

Figure 2:
Temporal comparison of annual mean PR (a) and annual SAT (b) among different datasets. Source [42]

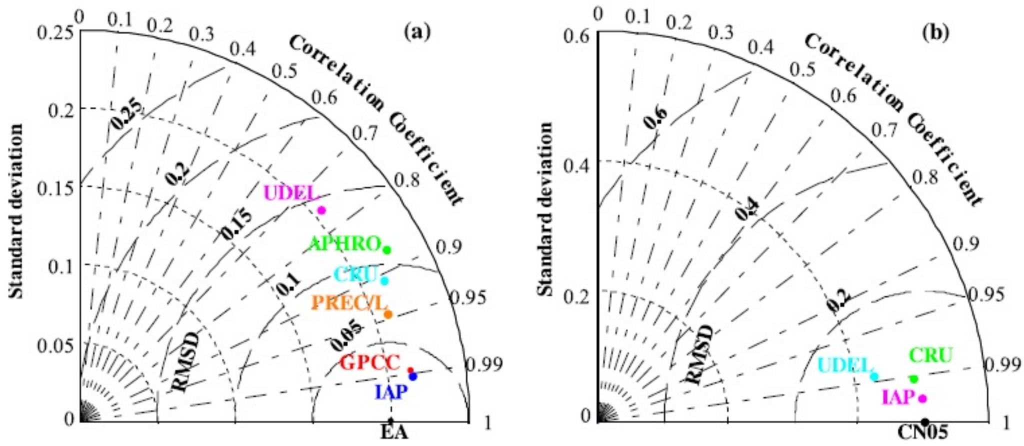

Figure 3:
The comparison among datasets based on Taylor diagrams ((a) PR; (b) SAT). Source [42].

to successful modelling in the cold regions of western China.

OTHER DATASETS

The access to other datasets needed for hydrological studies, e.g. DEM, soil type and characteristics, population growth rate, water demand, etc. is more difficult either because these data are available from local authorities, or they may be not updated, digitalised or their spatial resolution may be too low (e.g. DEM distributed by the National Geomatics Center of China has a resolution of 1:250,000, [17, 51]).

In Liu et al. [31] the digital elevation data was obtained from the USGS HYDRO1k data set; soil properties were obtained from the digital soil map of the world and derived soil properties on FAO's CD-ROM, whit a 5-minute resolution and the land cover was obtained from the USGS Global Land Cover Characteristics Data Base; those data were used to calibrate the TOPKAPI hydrological model.

In their study, Sun et al.[43] refer to the 90 m STRM (http://dds.cr.usgs.gov/srtm/) digital elevation model dataset to define watersheds boundaries and to the land-use/cover map provided by the Environmental and Ecological Science Data Center for West China, National Natural Science Foundation of China (http://westdc.westgis.ac.cn) with a spatial resolution of 1x1 km also used in [51] for SWAT2005 model.

MAIN RESULTS FROM STUDIES ON CLIMATE CHANGE OVER CHINA

Mostly of the cited works concentrates on the variation, i.e. abrupt changes or trend presence, of observed climate and/or hydrological variables over the whole Chinese territory or parts of it. Among the works focusing on climate changes in China, [37] analysed trend in observed climate and runoff data; [44] study the changes in climate of East Asia in the projection period (2021-2050) using A1B scenario with respect to (1971-2000); [24] focus on changes in cold temperature extremes using A1B scenario, with particular attention to cold waves duration and shifts in space; [55] concentrate in the variation of dryness/wetness conditions in ten large river basins under A1, A1B and B1 scenarios; [4] uses RCP4.5 and RCP8.5 scenarios to evaluate the precipitation according to climate projections from 16 CMIP5 models. The main results of each of this work are reported below.

In their work, *Piao et al.* [37] concentrate on climate change impacts on water availability, analysing observations of climate and river runoff trends in China, and try to derive an indication of climate change impacts on sustainability of the water demand. Through their analysis, Piao et al. evidences that climate in China has warmed since 1960 of about 1.2 °C, with an increased frequency of heatwaves Fig.4, and that glaciers are in retreat Fig.5. Climate warming is occurring faster in northern China than in southern, and climate projections show the same tendency. Precipitation show a different behaviour in northeastern China: decreasing of about 12% since 1960 and south China: increasing rainfall in summer and winter, see Fig.4. However, changes in precipitation are within the natural climate variability and not statistically significant. For northeastern China, the combination of decreasing precipitation and increasing temperature may result in a reduction of water availability. As example of the impacts of reduced precipitation and high water demand, Piao et al. present the Yellow river runoff, Fig.6. In contrast the Yangtze river shows a slightly positive trend in annual runoff, with reduction in autumn and increases in summer due to rainstorms that may

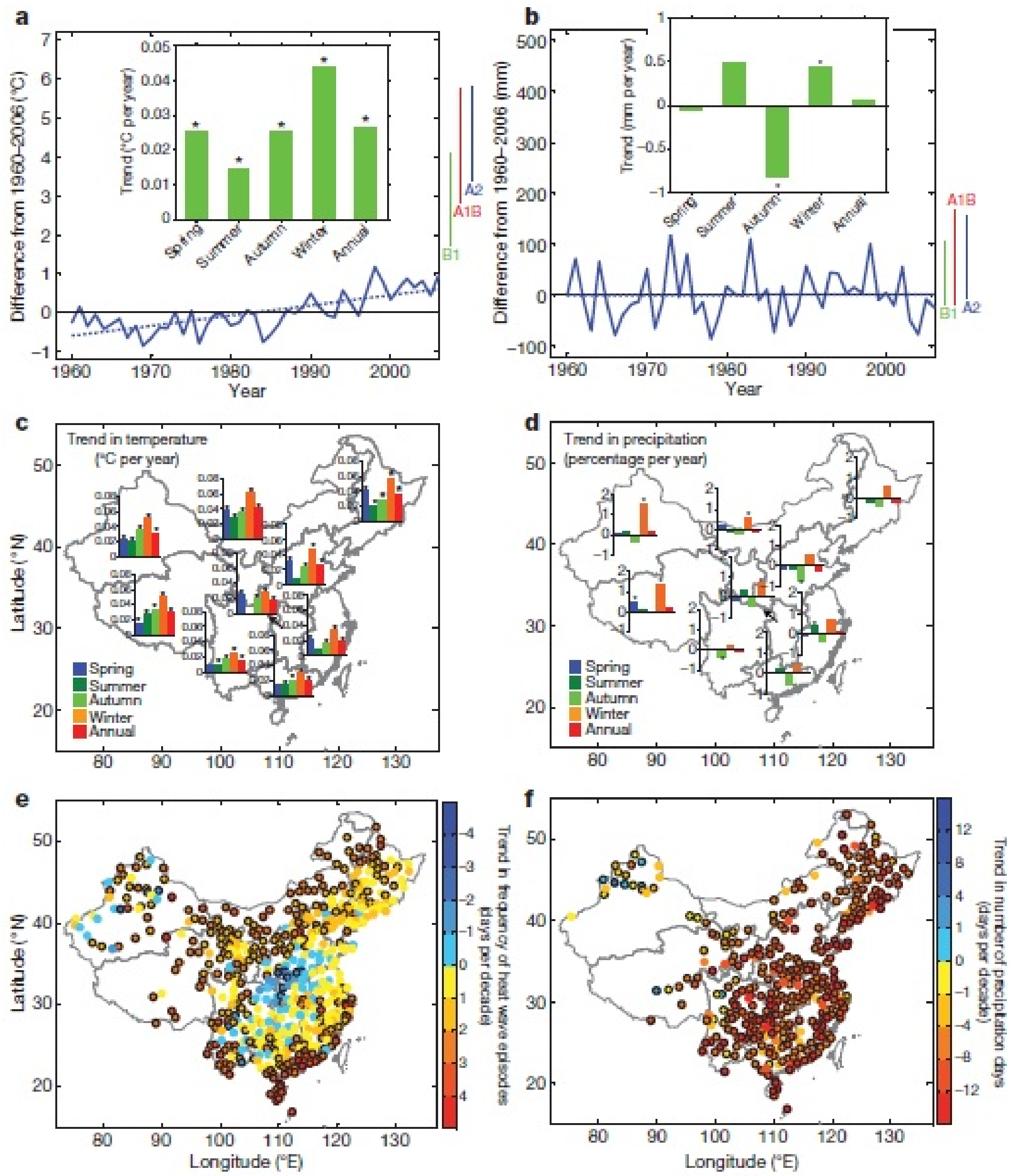

Figure 4:
Observed trends and future projections of climate in China. Climate of China in the 1960-2006 period. a, Observed mean annual temperature variations across the country, expressed as deviation from the mean during that period (blue line) an projected temperature range by 2100 for the three IPCC marker scenarios A1B, A2 and B1. The inset shows trends in seasonal temperature (°C per year). b, As for a but for precipitation variations. c, Spatial patterns of the trend in seasonal temperature (°C per year, shown as bar graphs). d, Spatial patterns of the trend in seasonal precipitation (percentage per year, shown as bar graphs). e, Spatial patterns of the trend in frequency of summer heatwave episodes (days per decade, shown as colour scale). f, Spatial patterns of the trend in rainfall days of precipitation occurrence (days per decade, shown as colour scale). Asterisks and black-edged circles indicates that the trend is statistically significant (P,0.05). Source [37].

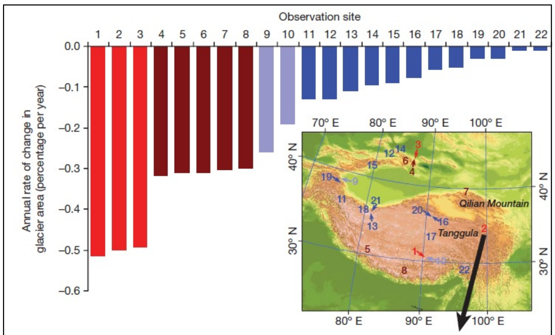

Figure 5:
Observed annual rate of change in glacier area at 22 monitoring stations in western China over the past 30-40 years. Negative rate indicates a shrinking glacier. Each glacier location is shown on the map inset. Source [37].

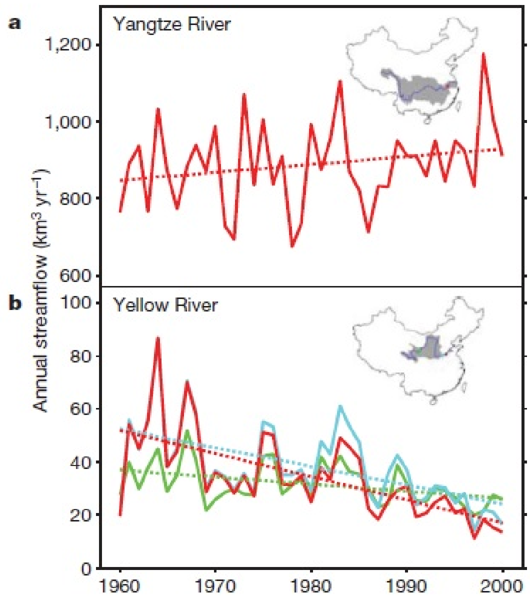

Figure 6:
Observed inter-annual variation in annual runoff in Yangtze and Yellow river. a, Observed inter-annual variation in the Yangtze River annual runoff at the Datong station (red dot on China map in inset; grey shading indicates the area of the Yangtze River basin) from 1960 to 2000. b, Observed inter-annual variation in the Yellow River annual runoff at the Lanzhou (upper basin), Huayuankou (lower basin), and Gaocun (lower basin) stations (green, blue and red dots on China map in inset; grey shading indicates the area of the Yellow River basin) from 1960 to 2000. Source [37].

cause flooding events, that will become more frequent if precipitation increases as projected. *Wang et al.* [44] study the changes in climate of East Asia in the projection period (2021-2050) with respect to (1971-2000). The area covered is about 10500 x 98000 skm and it includes China, Mongolia and most parts of India, Indochina and the islands of Indonesia, the Philippines, and Japan, the simulation grid is characterised by an horizontal resolution of 0.44°, Fig.7 reports the simulation domain. The continental area is divided into 17 sub-domains, shown in Fig.7, which were chosen according to Ko´oppen-Geiger classification and observed mean temperature and precipitation. The climate simulations are performed using the regional climate model COSMO-CLM driven by ERA-40 reanalysis data or by the global climate model ECHAM5. Wang et al. [44] validate the simulation with respect to CRU-TS 3.0 (Climate Research Unit 3) dataset for temperature, Fig.8, and APHRODITE dataset for precipitation. Figure 9 show that COSMO-CLM is able to reasonably capture the climate features of East Asia, including the monsoon dynamics on small scales, but a wet bias is present in the northern part of the domain, over the Tibetan Plateau, and over east Indonesia. The first column of Figs. 8 and 9 shows the temperature and precipitation bias of the ERA-40 driven COSMO-CLM run compared to CRU and APHRODITE datasets, respectively. The temperature bias ranges in most regions from -5 to 5 K with the exception of Himalaya and Karakorum regions where the bias ranges between -10 and 10 K. The extreme bias are located in the grid points characterised by a the steep orography that may not be reproduced adequately in COSMO-CLM. Wang et al. [44] find the strongest cold bias in the Tibetan Plateau and Indochina while the largest warm bias appears in the Tarim basin and western Mongolia; the cold bias in east Indonesia seems to be related to the overestimation of precipitation. Figure 9 shows the presence of a wet bias in the most northern part of the domain; over the Tibetan Plateau during the dry period (October to April) and over east Indonesia and the Philippines. Two ECHAM5-20C driven COSMO-CLM runs are used to assess the influence of natural forcing: ECHAM5-20C-R1 that account only for anthropogenic forcing and ECHAM5-20C-all-R3 that accounts for anthropogenic and natural forcing. The second and third columns of Fig.8 show that both ECHAM5-20C driven runs basically produce the same bias patterns as the ERA-40 driven run, few differences are detected in south India, Indochina and the north east continental areas (NEC and NE). The ECHAM5-20C driven simulations show in north-eastern area a temperature underestimation all over the year, while in south India a cold bias is detected in the summer. Over Indochina, the a slight overestimation of annual mean temperature is detected. There are no significant difference between temperature simulated by the two ECHAM5-20C driven simulations. About precipitation, the simulations driven by ECHAM5-20C driven are coherent with the one driven by ERA40, Fig.9. The strongest absolute biases in precipitation occur from March to August. In east Indonesia, the ECHAM5-20C driven runs perform better that the ERA-40 driven run, while in west Indonesia a more significant wet bias appears in the dry season (JJA) especially over the island of Java. Both ECHAM5-20C driven runs show again no significant difference. Wang et al. [44] simulates the future climate (2021-2050) under A1B scenario using both ECHAM5-20C driven COSMO-CLM, comparing the results with the respective past climate simulations. Results, for temperature, are reported in the last two columns of Fig.8 and of Fig.9 for precipitation. Both runs (only anthropogenic and anthropogenic plus natural forcing) produce an annual temperature increase of 1-2 K with a south to north gradient. Precipitation shows less systematic changes (Fig.9) but large differences between the two projections. The precipitation anomaly of the ECHAM5-A1B-R1 driven run is characterised by an increase of precipitation in a band around 20°N-50°N and a decrease elsewhere, with a significant decrease in the North China Plain and central and southern China in autumn while in summer the precipitation is projected to increase by more than 15% in west Indonesia, Indochina and south India. According to the ECHAM5-A1B-R3 driven run the Sichuan Basin will be subject to an increase of temperature and a decrease in precipitation; also China is projected to experience a 20% decrease in precipitation.

Jiang et al. [24] focus on changes in cold temperature extremes using A1B scenario, with particular attention to cold waves duration and shifts in space. A cold wave is defined as a spell of at least six consecutive days with minimum temperatures less than the local 10th percentile of the control period (1961-1990); and duration is identified with the duration of the longest cold wave per winter (November to February).

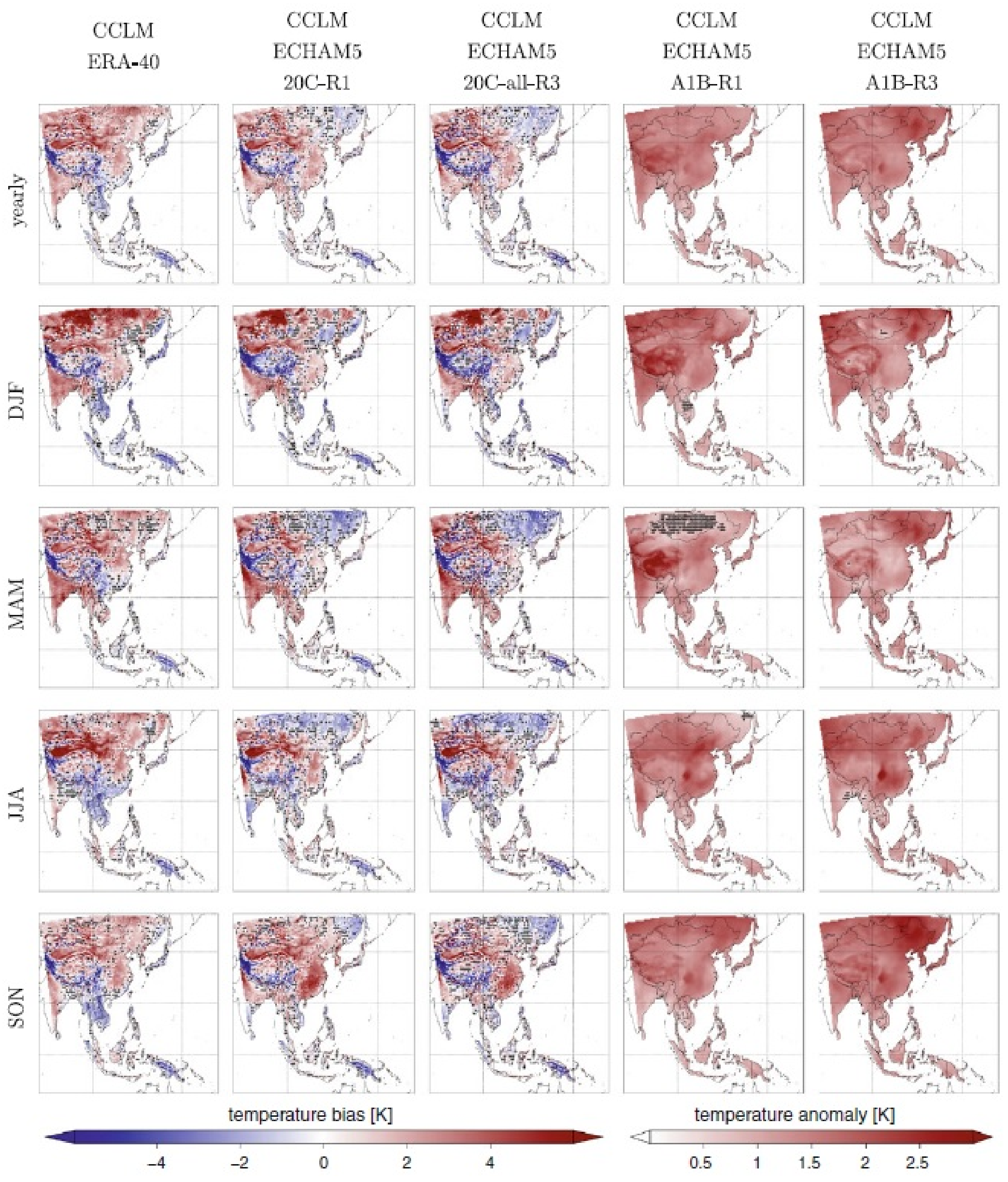

Figure 8:
The temperature bias of the five simulations. The control simulations over the period 1971-2000 are compared to CRU-TS3.0, while the future projections over the period 2021-2050 are compared to their respective control runs. Source [44].

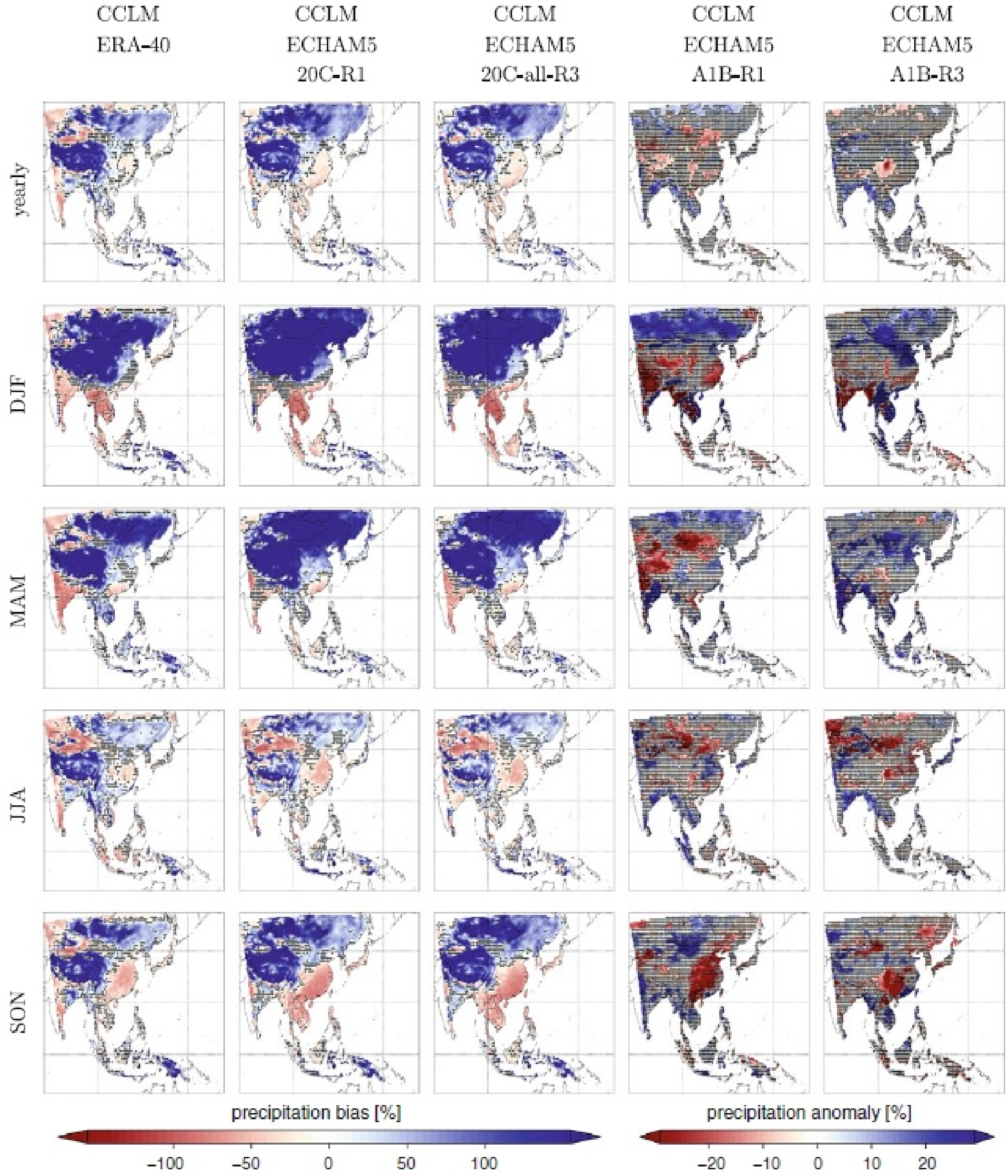

Figure 9:
The relative precipitation bias of the five simulations. The control simulations are compared to APHRODITE dataset, while the future projections over the period 2021-2050 are compared to their respective control runs. Source [44].

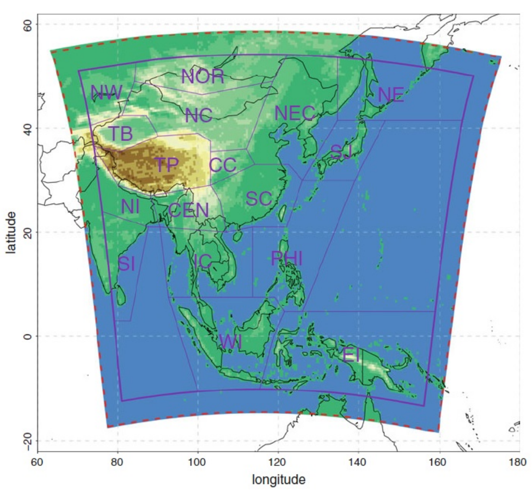

Figure 7:
The study region in [44]. Red dotted line: COSMO-CLM simulation domain; Solid purple line: evaluation region. Subregions: NW North West, NOR North, NEC North East China, NE North East, TB Tarim Basin, NC North China, CC Central China, SJ South Japan, TP Tibetan Plateau, SC South China, PHI Philippines, NI North India, SI South India, CEN Central, IC Indochina, WI West Indonesia and EI East Indonesia. Source [44].

Figure 10 provides the duration of cold waves in the 1957-1979 (cold period), in 1980-2009 (warm period) and the difference between the two periods. Jiang et al. [24] note that during the cold period the longest cold waves occur in north China and during the warm period in South China, and that the duration of cold waves in northern China is more variable than in southern China.

To assess the changes in cold waves duration at the end of the XXI century Jiang et al.[24] use a multi-model ensemble of seven climate models (ECHAM5/MPI-OM, MRICGCM2.3.2, CCCma-CGCM3.1 (T63), CNRM-CM3, CSIRO-Mk3.0, MIROC3.2-hires, and ECHAM4) under the IPCC SRES A1B scenario. Figure 11 shows the cold waves duration for the period 2080-2099 for each of the seven climate models considered. The climate models CCCma, MRI, MIROC, CSIRO and ECHAM4 project the ex-

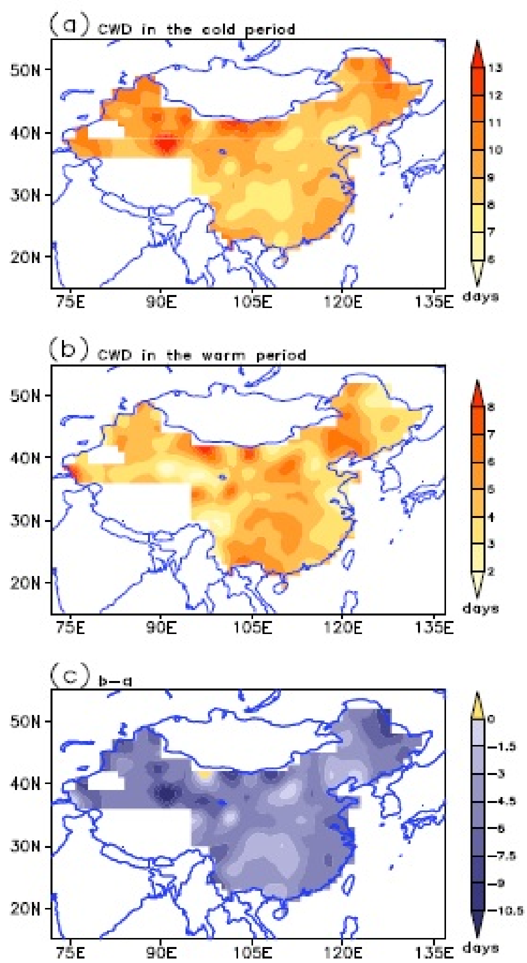

Figure 10:
The cold waves duration in (a) cold and (b) warm periods; (c) difference of the cold waves duration between the two periods (warm minus cold). Color shadings in unit of day. Source [24].

treme value centers of cold waves duration in southern China, while ECHAM5 and CNRM locate the maximum duration in northern China. As results, Jiang et al.[24] expect that by the end of XXI century the southern China will be subject to more prolonged cold waves.

Zhai et al. [55] investigates the variations in dryness/wetness within ten large river basins (Fig.12) in the first 50 years of the XXI century computing the SPI index, [33]. For the calculation of SPI they use average monthly precipitation data (2001-2050) of 3 runs for the A1B and B1 scenarios, and of the 4 runs for the A2 scenario from simulations of the GCM ECHAM5/MPI-OM by the Max Planck Institute for Meteorology. A month is considered dry if SPI<-1. According to Zhai et al. [55] results, in the period 2002-2050 under scenario A2 the areas characterised by the highest number of dry months will be North China, the Jinshajiang River catchment, the Hanjiang River catchment, the eastern part of the Huaihe River basin and the south part of the Pearl River basin. Considering the A1B scenario the areas more prone to dryness are located in the Songhuajiang River basin, the south part of Yellow River basin, the Jinshajiang River catchment, the Pearl River basin, the Southwest River basins and some parts of Northwest River basins. The Haihe River basin, the east part of Yellow River basin, the Dongting lake catchment of the Yangtze River basin, the Southeast River basins and some parts of Northwest River basins are the drier areas according to the B1 scenario. The spatial distribution of the number of dry months is reproduced in top panel of Fig.13, while on the bottom panel the spatial distribution of Mann-Kendall trend for the SPI timeseries is shown. For A2 scenario, a negative trend is evidenced from northeast to southwest China which covers the Songhuajiang River basin, the Liaohe River basin, the Haihe River basin, the Yellow River basin, the Upper reaches of the Yangtze River basin and the west part of Pearl River basin while positive trends are detected in the northwest and the southeast of China, including the northwest parts of the Inland River basins, the middle and lower Yangtze River basin and west of Qinghai-Tibet Plateau which covers part of the southeast River basins. For A1B scenario the area covered by a negative trend is reduced with respect to A1 scenario and it is detected in the Liaohe River basin, the river source region of the Yellow River and the Yangtze River, and the central Qinghai-Tibet Plateau which covers the southwest River basins and part of Northwest River basins; in some regions of the Dongting lake catchment and the Yangtze estuary. The trend of SPI in scenario B1 has shown a similar spatial distribution pattern with those of scenario A1B: the areas showing significant trends towards drier conditions are still located in northwest China and the upper reaches of the Yellow River, the Yangtze River and the southwest River. However considering areal averaged SPI index there is no evidence of specific trend towards dryness/wetness.

According to the work of *Chen et al.* [4] climate projections from 16 CMIP5 models covering the whole Chinese region shows a significant increase in the annual precipitation at the end of the 21st century compared to the present-day levels. The number of days and the intensity of medium (10-25 mm/d), large (25-50 mm/d) and heavy rain (>50 mm/d) are increased, while the number of trace rain (0.1-1.0 mm/d) days is projected to decrease over the entire area of China, Fig.14. The annual precipitation in northwest China is expected to increase due to the increase of light (1.0-10 mm/d) rain while the increases in north and northeast China are related to the increase of medium rain. In southern China, annual precip-

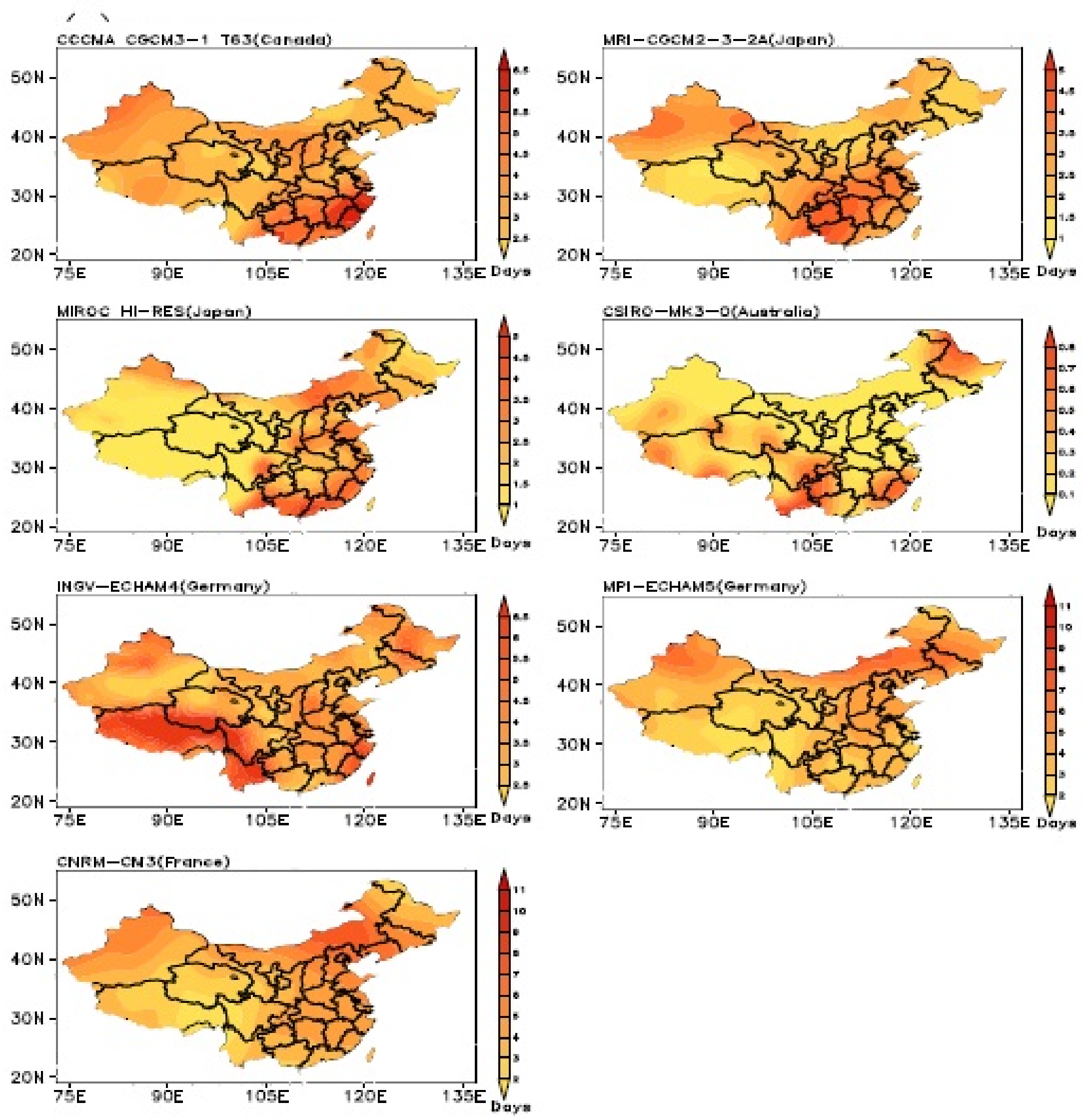

Figure 11:
Cold waves duration in winter across China within the period 2080-2099 from seven IPCC coupled models. Color shadings in unit of day. Source [24]

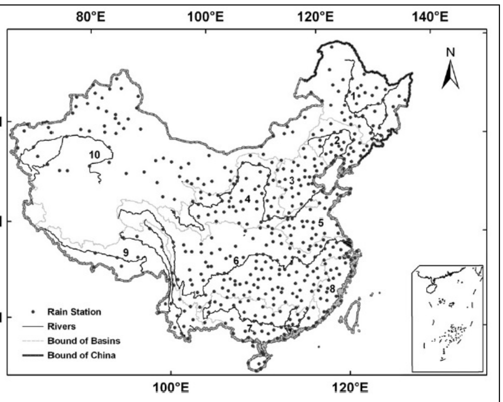

Figure 12:
Ten large river basins in China. Numbers denote the ten river basins: 1, the Songhuajiang River basin; 2, the Liaohe River basin; 3, the Haihe River basin; 4, the Yellow River basin; 5, the Huaihe River basin; 6, the Yangtze River basin; 7, the Pearl River basin; 8, the Southeast River basins; 9, the Southwest River basins; 10, the Northwest Inland River basins. Source [55].

...

itation increase would be linked to the increases of large rain and heavy rain, while light will reduce. The describe changes in the precipitation patterns are even more evident considering simulations under RCP8.5 scenario. Table 3 summarizes the expected changes for some features of medium, large and heavy rains under RCP4.5 and RCP8.5.

Additionally climate projections seems to indicate that the East Asian summer monsoon circulation would considerably stronger, and the local atmospheric stratification is projected to be more unstable, all of which provide a background benefit for the increase of precipitation and extreme rainfall events in China under climate change scenarios [4].

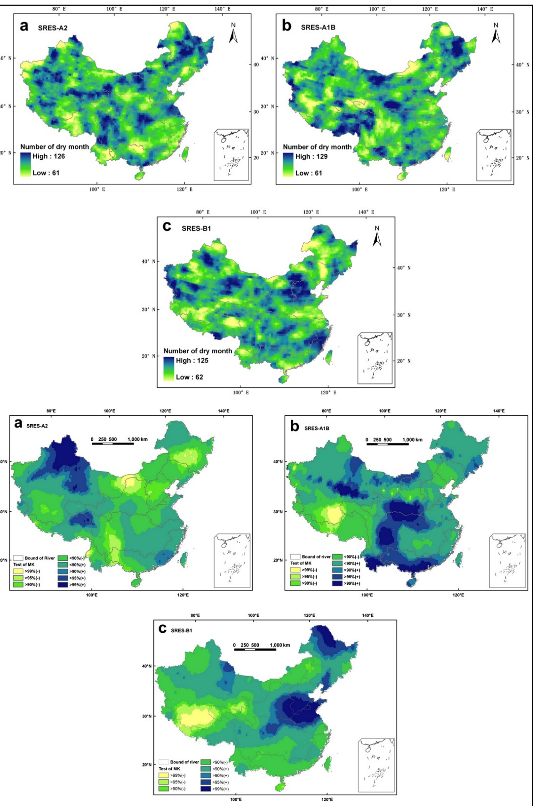

Figure 13:
For (a) scenario A2, (b) scenario A1B, (c) scenario B2, top: Number of dry months during 2002-2050 (588 months); bottom: trend of dryness/wetness. Source [55].

...

CONCLUSIONS

The Literature review evidences that high quality and long time series of observed climate variables are expected to be available from the

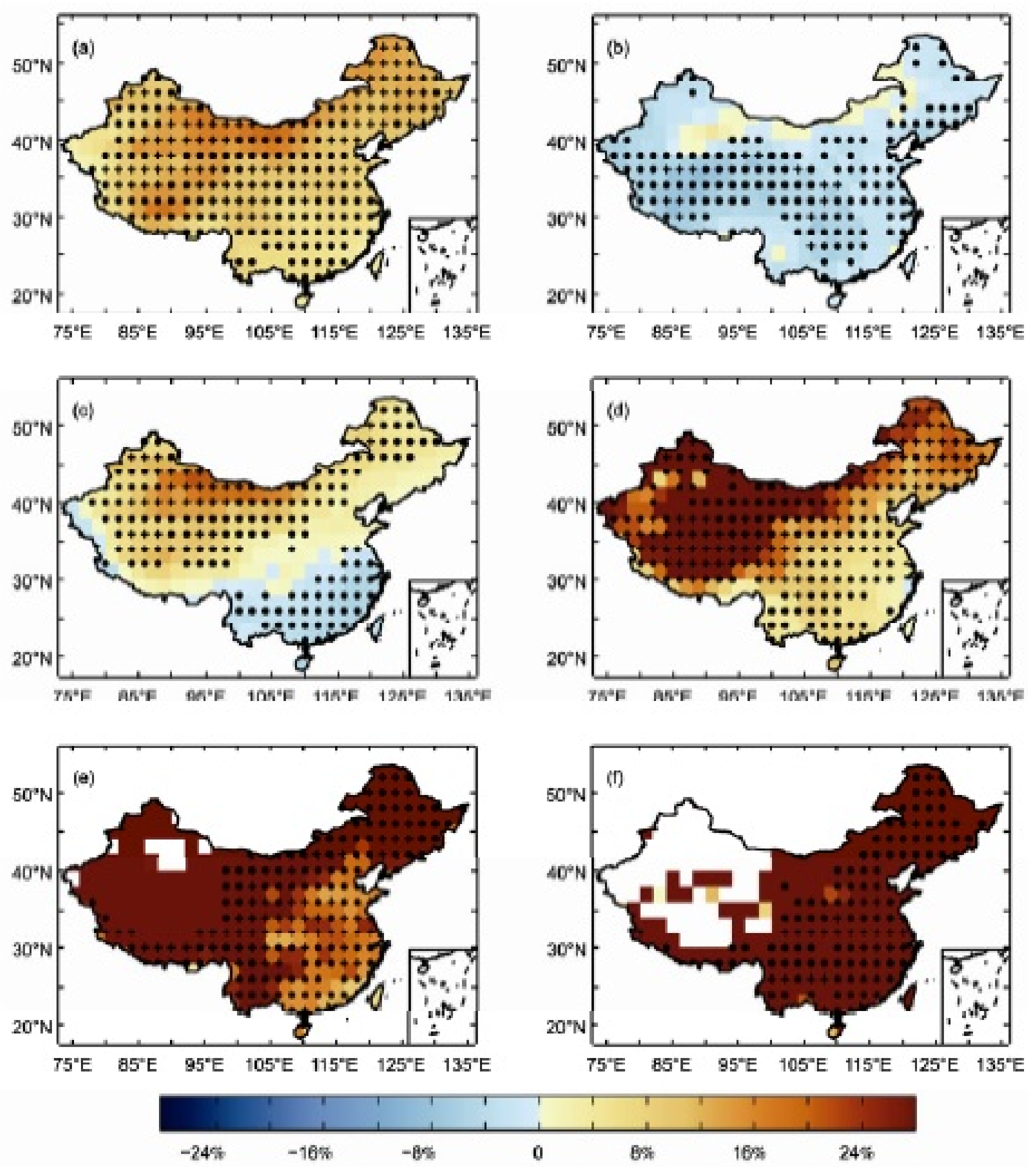

Figure 14:
Projected precipitation changes from the period of 1986-2005 to the period of 2080-2099 from the 16-model ensemble in the RCP4.5 scenario. (a) Annual precipitation, (b) trace rain, (c) light rain, (d) medium rain, (e) large rain, and (f) heavy rain. Dots: more than 67% (likely) of the models indicate a similar change as the multi model ensemble, and + shows at least 90% (very likely) of the models indicate such a change. Blank regions denote no rainy events. Source [4].

Table 3
Changes, in percentage, of medium, large and heavy rain at the end of XXI century based on results in [4]

	medium rain		large rain		heavy rain	
	RCP4.5	RCP8.5	RCP4.5	RCP8.5	RCP4.5	RCP8.5
Average Amount	12.0	16.7	31.6	35.0	62.9	153.7
N. of days	11.3	15.3	24.2	41.7	57.7	135.9
Intensity	3.4	6.5	10	18.3	44.7	98.8

National Climatic Centre of the China Meteorological Administration or from APHRODITE project. Alternatively, climate reanalysis from NCEP/NCAR or University of East Anglia are available to the scientific community. For discharge datasets, data are available from Hydrological Yearbooks or from the single Basin Authorities. As alternative, the runoff can be used to validate the hydrological cycle of the regional climate model, however, the resulting runoff may be closer to the natural one (i.e. in absence of water demand, lakes regulation, dams) than to the observed one, [3]. According to the literature review presented here, the number of sources from which climate datasets are available is superior to the number of sources for hydrological datasets. Climate change studies over China agree in projecting an increase in temperature while for precipitation and the results strongly depend on the climate scenario considered. Fro hydrological variables is even more complex to depict a clear picture since they are influenced not only by climate and anthropogenic forcing that may impact even more than climate changes.

Bibliography

[1] E. Bucchignani, P. Mercogliano, M. Montesarchio, A.L. Zollo, and M.P. Manzi. Prearrangement of the COSMO-CLM model on the chinese region and sensitivity analysis. *CMCC Reseach Paper*, (RP0136), 2012.

[2] E. Bucchignani, M. Montesarchio, P. Mercogliano, L. Cattaneo, and F. Cotroneo. Simulation of the period 1979-2011 over China with the regional climate model COSMO-CLM. *CMCC Reseach Paper*, (RP0181), 2013.

[3] L. Cao, W. Dong, Y. Xu, Y. Zhang, and S. Michael. Validating the runoff from the PRECIS model using a large-scale routing model. *Advances in Atmospheric Sciences*, 24(5):855–862, 2007.

[4] H.P. Chen. Projected change in extreme rainfall events in China by the end of the 21st century using CMIP5 models. *Chin Sci Bull*, 58:1462–1472, 2013.

[5] J. Chen, X. Wu, B.L. Finlayson, M. Webber, T. Wei, M. Li, and Z. Chen. Variability and trend in the hydrology of the Yangtze river, China: Annual precipitation and runoff. *Journal of Hydrology*, 513:403–412, 2014.

[6] M. Chen, P. Xie, and J. E. Janowiak. Global land precipitation: a 50-yr monthly analysis based on gauge observations. *J Hydrometeor*, 3:249–266, 2002.

[7] Y.D. Chen, Q. Zhang, X. Lu, S. Zhang, and Z. Zhang. Precipitation variability (1956-2002) in the Dongjiang river (Zhujiang river basin, China) and associated large-scale circulation. *Quaternary International*, 244:130–137, 2011.

[8] Y.D. Chen, Q. Zhang, C.-Y. Xu, X. Lu, and S. Zhang. Multiscale streamflow variations of the Pearl river basin and possible implications for the water resource management within the Pearl river delta, China. *Quaternary International*, 226:44–53, 2010.

[9] L. Cuo, Y. Zhang, Y. Gao, Z. Hao, and L. Cairang. The impacts of climate change and land cover/use transition on the hydrology in the upper Yellow river basin, China. *Journal of Hydrology*, 502:37–52, 2013.

[10] H. Deng, Y. Chen, X. Shi, W. Li, H. Wang, S. Zhang, and G. Fang. Dynamics of temperature and precipitation extremes and their spatial variation in the arid region of northwest China. *Atmospheric Research*, 138:346–355, 2014.

[11] M. Dong, Y. Jiang, D. Zhang, and Z. Wu. Spatio-temporal change in the climatic growing season in northeast China during 1960-2009. *Theor Appl Climatol*, 111:693–701, 2013.

[12] H. Du, Z. Wu, M. Li, Y. Jin, S. Zong, and X. Meng. Characteristics of extreme daily minimum and maximum temperature over northeast China, 1961-2009. *Theor Appl Climatol*, 111:161–171, 2013.

[13] X. Fan, Q. Wang, and M. Wang. Changes in temperature and precipitation extremes during 1959-2008 in Shanxi, China. *Theor Appl Climatol*, 109:283–303, 2012.

[14] F. Fang, J. Guo, L. Sun, J. Wang, and X. Wang. The effects of urbanization on temperature trends in different economic periods and geographical environments in northwestern China. *Theor Appl Climatol*, 116:227–241, 2014.

[15] T. Fischer, M. Gemmer, L. Lüliu, and S. Buda. Temperature and precipitation trends and dryness/wetness pattern in the Zhujiang river basin, south China, 1961-2007. *Quaternary International*, 244:138–148, 2011.

[16] X. Gao, Y. Shi, R. Song, F. Giorgi, Y. Wang, and D. Zhang. Reduction of future monsoon precipitation over China: comparison between a high resolution RCM simulation and the driving GCM. *Meteorol Atmos Phys*, 100:73–86, 2008.

[17] H. Guo, Q. Hu, and T. Jiang. Annual and seasonal streamflow responses to climate and land-cover changes in the Poyang lake basin, China. *Journal of Hydrology*, 355(1-4):106–122, 2008.

[18] Y. Hu, S. Maskey, and S. Uhlenbrook. Downscaling daily precipitation over the Yellow river source region in China: a comparison of three statistical downscaling methods. *Theor Appl Climatol*, 112:447–460, 2013.

[19] J. Huang, S. Sun, and J. Zhang. Detection of trends in precipitation during 1960-2008 in Jiangxi province, southeast China. *Theor Appl Climatol*, 114:237–251, 2013.

[20] J. Huang, J. Zhang, Z. Zhang, S. Sun, and J. Yao. Simulation of extreme precipitation indices in the Yangtze river basin by using statistical downscaling method (SDSM). *Theor Appl Climatol*, 108:325–343, 2012.

[21] F. Jiang, R. Hu, S.-P. Wang, Y. Zhang, and L. Tong. Trends of precipitation extremes during 1960-2008 in Xinjiang, the northwest China. *Theor Appl Climatol*, 111:133–148, 2013.

[22] F. Jiang, R. Hu, Y. Zhang, X. Li, and L. Tong. Variations and trends of onset, cessation and length of climatic growing season over Xinjiang, NW China. *Theor Appl Climatol*, 106:449–458, 2011.

[23] T. Jiang, Y.D. Chen, C. Xu, X. Chen, X. Chen, and V.P. Singh. Comparison of hydrological impacts of climate change simulated by six hydrological models in the Dongjiang basin, south China. *Journal of Hydrology*, 336:316–333, 2007.

[24] Z. Jiang, T. Ma, and Z. Wu. China coldwave duration in a warming winter: change of the leading mode. *Theor Appl Climatol*, 110:65–75, 2012.

[25] Ba. Li, Y. Chen, Z. Chen, and W. Li. Trends in runoff versus climate change in typical rivers in the arid region of northwest China. *Quaternary International*, 282:87–85, 2012.

[26] Z. Li, F. Zheng, W. Liu, and D.C. Flanagan. Spatial distribution and temporal trends of extreme temperature and precipitation events on the loess plateau of China during 1961-2007. *Quaternary International*, 226:92–100, 2010.

[27] L. Liang, L. Li, and Q. Liu. Precipitation variability in northeast China from 1961 to 2008. *Journal of Hydrology*, 404:67–76, 2011.

[28] J. Liu and R. Chen. Studying the spatio-temporal variation of snow-covered days over China based on combined use of MODIS snow-covered days and in situ observations. *Theor Appl Climatol*, 106:355–363, 2011.

[29] X. Liu, X. Dai, Y. Zhong, J. Li, and P. Wang. Analysis of changes in the relationship between precipitation and streamflow in the Yiluo river, China. *Theor Appl Climatol*, 114:183–191, 2013.

[30] Y. Liu, G. Huang, and R. Huang. Inter-decadal variability of summer rainfall in eastern China detected by the Lepage test. *Theor Appl Climatol*, 106:481–488, 2011.

[31] Z.-Y. Liu, B.-Q. Tan, X. Tao, and Z.-H. Xie. Application of a distributed hydrologic model to flood forecasting in catchments of different conditions. *Journal of Hydrologic Engineering*, 13(5):378–384, 2008.

[32] B. Mannig, M. MÃ$\frac{1}{4}$ller, E. Starke, C. Merkenschlager, W. Mao, X. Zhi, R. Podzun, D. Jacob, and H. Paeth. Dynamical downscaling of climate change in central Asia. *Global and Planetary Change*, 110:26–39, 2013.

[33] T.B. McKee, N.J. Doesken, and J. Kleist. tthe relationship of drought frequency and duration to time scales. In *Eighth Conference on Applied Climatology*, 1993.

[34] T.D. Mitchell and P.D. Jones. An improved method of constructing a database of monthly climate observations and associated high-resolution grids. *Int. J. Climatol.*, 25:693–712, 2005.

[35] M. New, M. Hulme, and P. Jones. Representing twentieth century space-time climate variability. part ii: development of 1901-96 monthly grids of terrestrial surface climate. *J. Clim.*, 13:2217–2238, 2000.

[36] State Council Information Office of China. *White paper: China's policies and actions on climate change*. available on line at http://China.org.cn/government/news/2008-10/29/content_16681689.htm, 2008.

[37] S. Piao, P. Ciais, Y. Huang, Z. Shen, S. Peng, J. Li, L. Zhou, H. Liu, Y. Ma, Y. Ding, P. Friedlingstein, C. Liu, K. Tan, Y. Yu, T. Zhang, and J. Fang. The impacts of climate change on water resources and agriculture in China. *Nature*, 467, 2010.

[38] B. Rockel, A. Will, and A. Hense. The regional climate model COSMO-CLM (CCLM). *Meteorologische Zeitschrift*, 17(4):347–348, 2008.

[39] B. Rudolf, A. Becker, U. Schneider, A Meyer-Christoffer, and M. Ziese. The new GPCC full data reanalysis version 5 2010. pages 1–7, 2009.

[40] Y.-F. Sang, Z. Wang, C. Liu, and J. Yu. The impact of changing environments on the runoff regimes of the arid heihe river basin, China. *Theor Appl Climatol*, 115, 2014.

[41] D. She, J. Xia, J. Song, H. Du, J. Chen, and L. Wan. Spatio-temporal variation and statistical characteristic of extreme dry spell in Yellow river basin, China. *Theor Appl Climatol*, 112:201–213, 2013.

[42] Q. Sun, C. Miao, Q. Duan, D. Kong, A. Ye, Z. Di, and W. Gong. Would the "real" observed dataset stand up? a critical examination of eight observed gridded climate datasets for China. *Environ Res Lett*, 9:169–183, 2014.

[43] S. Sun, H. Chen, W. Ju, J. Song, H. Zhang, J. Sun, and Y. Fang. Effects of climate change on annual streamflow using climate elasticity in Poyang lake basin, China. *Theor Appl Climatol*, 112:169–183, 2013.

[44] D. Wang, C. Menz, T. Simon, C. Simmer, and C. Ohlwein. Regional dynamical downscaling with cclm over east Asia. *Meteorol Atmos Phys*, 121:39–53, 2013.

[45] H. Wang, Y. Chen, S. Xun, D. Lai, Y. Fan, and Z. Li. Changes in daily climate extremes in the arid area of northwestern China. *Theor Appl Climatol*, 112:15–28, 2013.

[46] S. Wang and X. Zhang. Long-term trend analysis for temperature in the jinsha river basin in China. *Theor Appl Climatol*, 109:591–603, 2012.

[47] C.J. Willmott and K. Matsuura. Smart interpolation of annually annually averaged air temperature in the United States. *J. Appl. Meteorol.*, 34:2577–2586, 1995.

[48] S. Wu, A. Lu, and L. Li. Spatial and temporal characteristics of minimum temperature in winter in China during 1961-2010 from NCEP/NCAR reanalysis. *Theor Appl Climatol*, 108:207:216, 2012.

[49] M. Xiao, Q. Zhang, V.P. Singh, and X. Chen. Regionalization-based spatiotemporal variations of precipitation regimes across China. *Theor Appl Climatol*, 114, 2013.

[50] P. Xie, A. Yatagai, M. Chen, T. Hayasaka, Y. Fukushima, C. Liu, and S. Yang. A gauge-based analysis of daily precipitation over East Asia. *Journal of Hydrometeorology*, 8, 2007.

[51] H. Xu, R.G. Taylor, D.G. Kingston, T. Jiang, J.R. Thompson, and M.C. Todd. Hydrological modeling of river Xiangxi using SWAT2005: A comparison of model parameterizations using station and gridded meteorological observations. *Quaternary International*, 226, 2010.

[52] Y. Xu, Y. Gao, Y. Shen, C. Xu, Y. Shi, and F. Giorgi. A daily temperature dataset over China and its application in validating a RCM simulation. *Adv. Atmos. Sci.*, 26:763–772, 2009.

[53] A. Yatagai, O. Arakawa, M. I. Nodzu, K. Kamiguchi, H. Kawamoto, and A. Hamada. A 44 year daily gridded precipitation dataset for Asia based on a dense network of rain gauges. *Sola*, 5:137–140, 2009.

[54] A. Yatagai, K. Kamiguchi, O. Arakawa, A. Hamada, N. Yasutomi, and A. Kitoh. APHRODITE constructing a long-term daily gridded precipitation dataset for Asia based on a dense network of rain gauges. *BAMS*, 2012.

[55] J.Q. Zhai, B. Liu, H. Hartmann, B.D. Su, T. Jiang, and K. Fraedrich. Dryness/wetness variations in ten large river basins of China during the first 50 years of the 21st century. *Quaternary International*, 226:101–111, 2010.

[56] Q. Zhang, J. Li, Y.D. Chen, and X. Chen. Observed changes of temperature extremes during 1960-2005 in China: natural or human-induced variations? *Theor Appl Climatol*, 106:417–431, 2011.

[57] Q. Zhang, C. Liu, C.-Y. Xu, Y. Xu, and T Jiang. Observed trends of annual maximum water level and streamflow during past 130 years in the Yangtze river basin, China. *Journal of Hydrology*, 324:255–265, 2006.

[58] Q. Zhang, J. Peng, C.-Y. Xu, and V.P. Singh. Spatiotemporal variations of precipitation regimes across Yangtze river basin, China. *Theor Appl Climatol*, 115:703–712, 2014.

[59] Q. Zhang, C.-Y. Xu, Z. Zhang, Y.D. Chen, C. Liu, and H. Lin. Spatial and temporal variability of precipitation maxima during 1960-2005 in the Yangtze river basin and possible association with large-scale circulation. *Journal of Hydrology*, 353:215–227, 2008.

[60] S. Zhang, X. Gao, B. Ye, X. Zhang, and S. Hagemann. A modified monthly degree-day model for evaluating glacier runoff changes in China. Part II: application. *Hydrol Process*, 26:1697–1706, 2012.

[61] W. Zhang, Y. Yan, J. Zheng, L. Li, X. Dong, and H. Cai. Temporal and spatial variability of annual extreme water level in the Pearl river delta region, China. *Global and Planetary Change*, 69:35–47, 2009.

[62] X. Zhang and X. Yan. Temporal change of climate zones in China in the context of climate warming. *Theor Appl Climatol*, 115:167–175, 2014.

[63] G. Zhao, X. Mu, G. Hörmann, N. Fohrer, M. Xiong, B. Su, and X. Li. Spatial patterns and temporal variability of dryness/wetness in the Yangtze river basin, China. *Quaternary International*, 282, 2012.

[64] T. Zhao, W. Guo, and C. Fu. Calibrating and evaluating reanalysis surface temperature error by topographic correction. *J. Clim.*, 21:1440–1446, 2008.

[65] J. Zhou, J.W. Pomeroy, W. Zhang, G. Cheng, G. Wang, and C. Chen. Simulating cold regions hydrological processes using a modular model in the west of China. *Journal of Hydrology*, 509:13–24, 2014.